Global hydration kinetics of tricalcium silicate cement

F. Tzschichholz[1,2,3] and H. Zanni[3]
[1]*Institut für Computeranwendungen I, Universität Stuttgart, Pfaffenwaldring 27, D-70569 Stuttgart, Germany*
[2]*Department of Physics, Norwegian University of Science and Technology, N-7034 Trondheim, Norway*
[3]*Laboratoire de Physique et Mécanique des Milieux Hétérogènes (CNRS, URA 857), Ecole Supérieure de Physique et de Chimie Industrielle de la Ville de Paris, 10 Rue Vauquelin, 75231 Paris Cedex 05, France*
(Received 29 January 2001; published 19 June 2001)

We reconsider a number of measurements for the overall hydration kinetics of tricalcium silicate pastes having an initial water to cement weight ratio close to 0.5. We find that the time dependent ratio of hydrated and unhydrated silica mole numbers can be well characterized by two power laws in time, $x/(1-x) \sim (t/t_\times)^\psi$. For early times $t<t_\times$ we find an ''accelerated'' hydration ($\psi=5/2$) and for later times $t>t_\times$ a parabolic behavior ($\psi=1/2$). The crossover time is estimated as $t_\times \approx 16$ h. We interpret these results in terms of a global second-order rate equation indicating that (a) hydrates catalyze the hydration process for $t<t_\times$, (b) they inhibit further hydration for $t>t_\times$, and (c) the value of the associated rate constant is of magnitude 6×10^{-7}–7×10^{-6} l mol^{-1} s^{-1}. We argue, by considering that the hydration process actually occurs via diffusion limited precipitation, that the exponents $\psi=5/2$ and $\psi=1/2$ directly indicate a preferentially platelike hydrate microstructure. This is essentially in agreement with experimental observations of cellular hydrate microstructures for this class of materials.

DOI: 10.1103/PhysRevE.64.016115 PACS number(s): 82.40.Ck, 81.30.Mh, 61.43.−j, 81.05.Rm

I. INTRODUCTION

Heterogeneous solid-state transformations are of great importance and practical interest in industrial and technological applications. Perhaps the most prominent examples are transformations within alloys and steels playing a crucial role in their mechanical and durabillity properties. Solid-state transformations are frequently accompanied by microstructural changes within the material in the form of phases precipitating (segregating) from (solid) solutions. In its simplest form the transformation takes place between a major component acting as a solvent and an initially solvated phase. The precipitation process of the solvated phase is usually considered to happen in three main stages; phase nucleation, phase growth, and finally a coarsening process leading to a homogenization of microstructural geometrical properties [1,2]. Below we will employ basic concepts of solid-state transformation in order to interpret the experimentally observed hydration kinetics of cement (see Sec. III).

The massive introduction of hydraulic binders into daily engineering problems indicates the importance of a better understanding of how these materials work. Moreover, cementing processes are also of great importance for certain geological problems, e.g., for the formation, properties, and behavior of sedimentary basins [3]. Typical hydraulic binders are plaster, cement, mortar, and concrete. In the following we will focus more closely on the hydration of pure Portland cement (tricalcium silicate).

Basic phenomenological aspects of cement hydration can be characterized as follows. Initially fine grained cement powder (here tricalcium silicate, $C_3S \equiv Ca_3SiO_5$, with grain diameters typically ranging between 5 μm and 50 μm [4]) is mixed well with water. Tricalcium silicate is a well crystallized compound ($\rho=3.21$ g cm^{-3}) and the powders employed typically have specific surface areas 3×10^3 cm^2 g^{-1} [5]. After mixing the cement particles start to dissolve rapidly. The principal reaction products are solvated ions (Ca^{2+}, OH^-, and $H_2SiO_4^{2-}$) diffusing within the solvent. The ion concentrations are bounded by finite solubility products above which hydrate phases start to precipitate from solution, preferably on surfaces of already existing hydrates. There are two associated hydrates, (a) the cement hydrate [$C_{1.5}SH_{2.5} \equiv (CaO)_{1.5}\ (SiO_2)\ (H_2O)_{2.5}$] and (b) the Portlandite [$CH \equiv Ca(OH)_2$], which compete for the common calcium and hydroxyl ions. The cement hydrate ($\rho=2.35$ g cm^{-3}) is amorphous in contrast to the crystalline Portlandite ($\rho=2.24$ g cm^{-3}).

The process of cement dissolution, ion diffusion, and hydrate precipitation is usually referred as ''cement hydration.'' The ion diffusion represents the physical coupling between the chemical dissolution and precipitation reactions leading to a complex physicochemical evolution of hydrate microstructure.

In Fig. 1 we show a hydrated microstructure after 40 h of hydration time. The leaf/foil-like structure is typical.

In the following we will propose an empirical global reaction rate law for the hydration of cement pastes for initial water to cement weight ratios $w/c=0.5$, which is based on already published NMR measurements. The observed values for the kinetics exponents can be understood—in part—by classical solid-state transformation theory.

II. EXPERIMENTAL RESULTS AND KINETIC RELATIONSHIPS

The hydration of cement is spontaneous (exothermic) and irreversible and can be characterized by the *global* net reaction [5,6]

$$C_3S_{(s)} + 4H_2O_{(\ell)} \xrightarrow{k} C_{1.5}SH_{2.5(s)} + 1.5CH_{(s)}, \qquad (2.1)$$

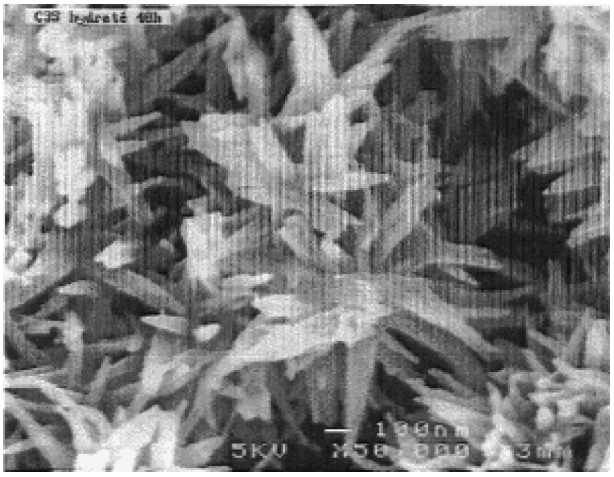

FIG. 1. Scanning electron micrograph of hydrated tricalcium silicate cement after 40 h hydration time. The initial water to cement ratio was 0.5. Note the leaflike hydrate microstructure. (Reproduced by courtesy of Institute Francais du Petrole.)

where k denotes an effective rate constant characterizing the solid to solid conversion rate. Because Eq. (2.1) describes a net reaction originating from various subprocesses the stoichiometric numbers in Eq. (2.1) are not related to the kinetic exponents of the overall reaction rate law. The kinetics of cement hydration has been experimentally studied to some extent by calorimetric and conductimetric measurements [5,7], by x-ray diffraction [8,9], by Raman spectroscopy [10], and by NMR spectroscopy [11–14].

A. NMR measurements

^{29}Si NMR spectroscopy has been used to experimentally determine the CSH growth rate [11–14]. The method employed [single pulse excitation with magic angle spinning (MAS/SPE)] is based on the fact that in the NMR spectrum the signal of the C_3S silicon nuclei (monomer) is separated from those of CSH silicon nuclei (dimers and trimers) [15]. The distinction between dimer (silicon chain ends) and trimer (inside silicon chains) signals has been used to investigate the polymerization process within the cement hydrate; see for example Ref. [12].

In order to enhance the signal/noise ratio one generally needs to sample the NMR signal. In order to obtain quantitative information about the populations of the different chemical species present in the specimen, one needs to strictly respect the relaxation of each population between successive samplings. We checked that the NMR data employed [11–13] meet this condition. NMR signal intensities I_k are in general proportional to the absolute number n_k of excited silicon nuclei of species k within the sample, $I_k = \Gamma n_k$, with Γ being the constant of the measurement (species k denotes a silicon nucleus belonging to a monomer, dimer, or trimer silicon cluster). The proportionality constant is usually eliminated by considering relative signal intensities $I_k/\Sigma_j I_j$ which correspond to mole fractions $x_k = n_k/\Sigma_j n_j$. The constant $\Sigma_j n_j$ defines the absolute silicon mass scale. The NMR measurements provide plots of the time dependent mole fractions for monomer, dimer, and trimer silicon nuclei [11–13]. However, plots for mole fractions show more complex algebraic behavior as will be demonstrated below.

B. Schematic representation

In order to get an idea about the global hydration kinetics of cement we consider the chemical *net* reaction (2.1) in a more schematic representation,

$$A \overset{k}{\rightharpoonup} B, \tag{2.2}$$

where the species A and B refer to silicon nuclei of C_3S and CSH respectively. We denote the anhydrous C_3S (monomer) mole fraction as $x_A(t)$ and the CSH (dimer as well as trimer) mole fraction as $x_B(t)$, i.e., $x_A(t)+x_B(t)=1$.

One should say something about the range of validity, the similarities, and the differences of Eqs. (2.1) and (2.2). Strictly speaking, the above net reactions can hold only if the employed water to cement weight ratio is not too high, that is to say, the number of solvated ions should always be orders of magnitude lower than the number of molecules belonging to the solid state, i.e., Eqs. (2.1) and (2.2) are inconsistent in the limit of infinite dilution. An approximate condition follows from a comparison of the cement to water concentration with the solubility of Portlandite, S_{CH}, $n_{C_3S}(t_0)/V_{H_2O}(t_0) \gg S_{CH} \approx 2\times 10^{-2}$ mol l^{-1}, or $w/c \ll 200$. The experimental data considered here certainly fulfill this condition, i.e., $w/c \approx 0.5$.

Furthermore, Eq. (2.1) describes a solid-liquid to solid transformation, but Eq. (2.2) a solid to solid transformation. It is thus natural that the two reactions describe very different things, if the initial water to cement ratio is so low that the water becomes a severely limiting reactant for the hydration process (case of very thick pastes). To be more specific, the hydration following Eq. (2.1) cannot be completed for chemical reasons if $4n_{C_3S}(t_0) > n_{H_2O}(t_0)$ or equivalently if $w/c < (w/c)^* = 0.31$. It is difficult to judge *a priori* whether the employed experimental water/cement ratio $w/c=0.5$ is sufficiently large to exclude a systematic effect on hydration due to limiting water. However, as we will see below, considering the kinetics of the deacceleration/parabolic period, water is very unlikely to be a chemically limiting reactant. However, it is not possible to determine from the considered measurements any water-specific kinetic exponent for the associated rate law of Eq. (2.1). The determination of such a dependency would require a set of experiments conducted for different initial water to cement ratios. Similarly, it is not possible to determine kinetic exponents for Portlandite (CH) from the considered measurements, because n_{CSH} is directly proportional to n_{CH} at every instant. In order to isolate the kinetic influence of precipitated Portlandite on the overall hydration kinetics one needs to split up the direct proportionality between n_{CSH} and n_{CH}. Preferably this could be done by examination of the hydration rate dependence for different initial CH admixtures, i.e., $n_{CH}(t_0) > 0$. Bearing the foregoing caveats in mind, it should be obvious why we consider

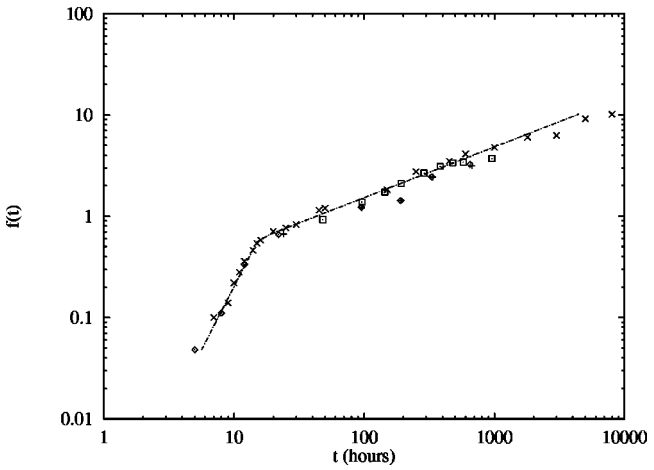

FIG. 2. Double-logarithmic plot of the measured mole ratio between hydrated and unhydrated silicon $f(t)=x_B/(1-x_B)$ as a function of hydration time t employing NMR and TGA (thermogravimetric analysis). All measurements correspond to a water to cement weight ratio $w/c=0.5$ conducted at room temperature and normal pressure. The data are well represented by two power laws: for $t<t_\times$ by Eq. (2.4) ($\gamma=2.5$) and for $t>t_\times$ by Eq. (2.5) ($\delta=0.5$). The dashed line shows the corresponding numerical fit according to Eq. (2.6) employing $t_\times=16$ h, $f(t_\times)=0.6$, and $m=20$. Data from ($\diamond$) Ref. [11] (NMR), ($\times$) Ref. [12] (NMR), ($\square$) Ref. [13] (NMR), and ($+$) Ref. [11] (TGA).

the schematic reaction (2.2). We are in a position to characterize only the kinetic influence of reactants and products on cement hydration. In our opinion even this limited information will be useful.

C. Kinetic relationships

We consider the ratio of silicon mole fractions,

$$f(t)=x_B(t)/x_A(t), \tag{2.3}$$

varying between 0 (no hydrates at time $t=0$) and ∞ (complete hydration at time $t=\infty$). Figure 2 shows a double-logarithmic plot of $f(t)$ versus the hydration time. This figure reveals several interesting facts about the hydration kinetics which will be addressed in this paper. The experimental data considered were taken from three independent publications obeying similar experimental conditions (room temperature, normal pressure, geometry of specimens, and initial water/cement weight ratio $w/c=0.5$); see [11–13] for details. The relatively narrow scatter of the data over order of magnitudes demonstrates consistent and reproducible measurements.

We observe, within the scatter, two power laws separated by a sharply defined characteristic time $t_\times=16$ h with value $f_\times\equiv f(t_\times)=0.6$. For the early hydration period ($t<t_\times$) we obtain

$$f(t)=f_\times\left(\frac{t}{t_\times}\right)^\gamma, \tag{2.4}$$

with an exponent $\gamma=2.5$. Below 5 h of hydration time there are no quantitative NMR data available, because of the bad signal/noise ratio for *CSH*. After $t_\times=16$ h the hydration dramatically slows down,

$$f(t)=f_\times\left(\frac{t}{t_\times}\right)^\delta, \tag{2.5}$$

with $\delta=0.5$. This second period is from 16 h to at least 8×10^3 h of hydration time. Equations (2.4) and (2.5) define a continuous dependency in time. However, the first derivative of $f(t)$ taken at $t_\times$ is not continuous, which might appear unphysical. The discontinuity in df/dt arises because we have assumed a zero crossover range in Eqs. (2.4) and (2.5) to obtain the best representation of experimental data. It is interesting to note that an ansatz of the form

$$t/t_\times=2^{-1/m}[(f/f_\times)^{\alpha m}+(f/f_\times)^{\beta m}]^{1/m} \tag{2.6}$$

with properly chosen exponents $\alpha=0.4$ and $\beta=2.0$ gives a quite satisfactory representation of the data for high integers m; see Fig. 2 [16]. The best representation is found for $m\to\infty$, which corresponds to Eqs. (2.4) and (2.5).

In the following we propose relations between the above mentioned exponents γ and δ and the kinetic exponents of an overall rate equation. The observed exponents will lead to some general statements about the hydration mechanisms.

From Eq. (2.3) the trivial relations

$$x_A(t)=\frac{n_A(t)}{n_A(t_0)}=\frac{1}{1+f(t)} \tag{2.7}$$

and

$$x_B(t)=\frac{n_B(t)}{n_A(t_0)}=\frac{f(t)}{1+f(t)} \tag{2.8}$$

are obtained, where $n_A(t_0)$ characterizes the absolute silicon mass scale. The overall rate equation for x_A and x_B has to be first order in time,

$$-\frac{d}{dt}x_A=\frac{d}{dt}x_B=\frac{1}{(1+f)^2}\frac{d}{dt}f. \tag{2.9}$$

One particular observation from Eqs. (2.7), (2.8), and (2.9) is that the global hydration rate can be represented as a product of powers of the mole fractions x_A and x_B, if df/dt follows a power law in f. In this case the reaction is of overall order 2 and $f(t)$ follows a power law in time, except for $df/dt\sim f$ which yields an exponential dependency in time. We have already mentioned, considering the experimental results in Fig. 2, that $f(t)$ follows two power laws, Eqs. (2.4) and (2.5), separated by a characteristic time $t_\times$. Thus it is possible to extract two rate laws from the measurements; one for early times $t<t_\times$ and another one for late times $t>t_\times$. Consider $f(t)=f_\times\times(t/t_\times)^\psi$ where for times $t<t_\times\psi=\gamma$ and for times $t>t_\times\psi=\delta$, according to Eqs. (2.4) and (2.5). The associated first-order differential equation is $(d/dt)f=\psi t_\times^{-1}f_\times^{1/\psi}f^{(\psi-1)/\psi}$. Inserting this into Eq. (2.9) and resort-

ing with respect to the factors x_B and x_A [Eqs. (2.8) and (2.7)] we obtain the explicit rate equation in terms of mole fractions,

$$-\frac{d}{dt}x_A=\frac{d}{dt}x_B=\psi t_\times^{-1}f_\times^{1/\psi}x_B^{(\psi-1)/\psi}x_A^{(\psi+1)/\psi}, \quad (2.10)$$

with $\psi=2.5$ for $t<t_\times$ and $\psi=0.5$ for $t>t_\times$.

Furthermore, by passing from mole fractions to concentrations, it is possible to determine the approximate effective rate constant(s) from the experimentally observed crossover point, the extracted exponents, and the initial water to cement weight ratio. It is convenient to consider first the initial concentration $[A]|_{t_0}=n_A(t_0)/V_0$ of cement in the overall specimen volume $V_0=V_{C_3S}(t_0)+V_{H_2O}(t_0)$ [17],

$$\frac{1}{[A]|_{t_0}}=\left(1+\frac{\rho_{C_3S}}{\rho_{H_2O}}\frac{w}{c}\right)v_{C_3S}\approx 0.18 \ \mathrm{l\,mol^{-1}}, \quad (2.11)$$

with $\rho_{C_3S}/\rho_{H_2O}=3.21$ and $v_{C_3S}=7.2\times10^{-2}$ $\mathrm{l\,mol^{-1}}$ being the relative density and the molecular volume of cement, respectively. The considered water to cement weight ratio is $w/c=0.5$.

We find for the accelerated period ($t<t_\times$)

$$-\frac{d}{dt}[A]=\frac{d}{dt}[B]=k_{t<t_\times}[B]^{0.6}[A]^{1.4}, \quad (2.12)$$

with $k_{t<t_\times}=2.5[A]|_{t_0}^{-1}t_\times^{-1}f_\times^{0.4}\approx 7\times10^{-6}$ $\mathrm{l\,mol^{-1}\,s^{-1}}$, and for the deaccelerated period ($t>t_\times$)

$$-\frac{d}{dt}[A]=\frac{d}{dt}[B]=k_{t>t_\times}[B]^{-1.0}[A]^{3.0}, \quad (2.13)$$

with $k_{t>t_\times}=0.5[A]|_{t_0}^{-1}t_\times^{-1}f_\times^{2.0}\approx 6\times10^{-7}$ $\mathrm{l\,mol^{-1}\,s^{-1}}$.

III. INTERPRETATION

Before we present a possible explanation for the hydration kinetics as manifested in Eqs. (2.12) and (2.13) we would like to give a brief account of another representation of the hydration kinetics that is more widespread in cement literature, i.e., the degree of hydration $\alpha(t)$. The degree of hydration is usually referred to as the relative amount (mole fraction) of hydrated cement [18], $\alpha(t)\equiv x_B(t)=1-x_A(t)$. Therefore Eq. (2.8) gives the relationship between $\alpha(t)$ and $f(t)$ as defined in Eq. (2.3). Typical experimental curves for the degree of hydration exhibit sigmoidal shapes in linear representations. However, the observed inflection points generally do not have any particular significance for a change in chemical mechanism. This can be seen, for example, by assuming in Eq. (2.10) $\Psi>1$ for *all times*. The degree of hydration will show an inflection point although there is only a single chemical mechanism (rate law) operative. Therefore it is not reliable to read off characteristic times from $\alpha(t)$ diagrams. While $\alpha(t)$ approximates $f(t)$ well if $f\ll1$ (early hydration) the discrepancy becomes very large for $f\gg1$ (late hydration).

The foregoing remark has hopefully illustrated why we have avoided degree of hydration diagrams in our considerations. As another motivation for our approach we present in Fig. 3 a so-called Avrami plot for the hydrated silicon amount, i.e., a test of the stretched exponential relationship $x_B=1-\exp[-(t/\tau)^k]$. Such empirical relationships are frequently found for overall transformations [1]. It can be clearly seen from Fig. 3 that the hydration data cannot be described by such a relation.

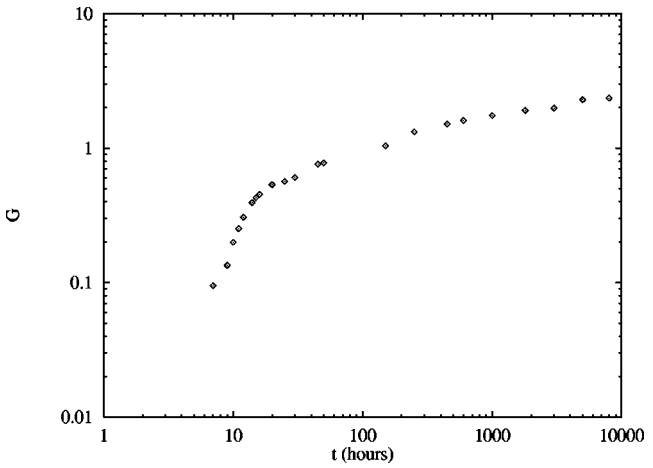

FIG. 3. Avrami plot for the amount of hydrated silicon [double-logarithmic plot of the negative logarithm of amount of unhydrated silicon $G=-\log_{10}(x_A)$ versus time t]. If the hydration kinetics followed a generalized Avarami-Johnson-Mehl law, i.e., $x_A=1-x_B=\exp[-(t/\tau)^k]$, the data should lie on a single straight line of slope k. It can been seen that this is not the case. The data were taken from Ref. [12] (NMR).

Before giving an interpretation of our findings we would like to briefly comment on Knudsen's dispersion model [24] and the connection to our results. The dispersion model is constructed by looking at the global degree of hydration $\alpha(t)$ expressed in terms of a linear convolution of the particle-size distribution of cement grains $w(r)$ and the degree of hydration $\alpha(r,t)$ of a particle of radius r at time t. The model assumes that the hydration processes of the individual grains do not interfere with each other. Then under the assumption of certain particle-size distributions (exponential) and certain $\alpha(r,t)$ (exponential) the global hydration ratio $f(t)$ satisfies a quadratic equation for arbitrary times, i.e., $t_0+t_1f(t)+t_2f^2(t)=t$. Such a quadratic equation was employed in Knudsen's work [24] in order to fit experimental data. Knudsen's formula predicts $f\sim t$ for early times, and $f\sim\sqrt{t}$ for late times [cf. Eq. (2.6)]. In contrast to this we observe for early times 5/2 as exponent, and furthermore we do not see a broad transition into parabolic growth as is expected from the quadratic equation. We see a rather sharp transition and we will discuss further below why there is good reason to believe that this is a morphological transition.

The kinetic equations Eqs. (2.12) and (2.13) allow one to make more substantial statements about the global cement hydration mechanism(s). During the acceleration period already existing hydrates catalyze the precipitation of new hydrates [positive kinetic exponent for the products in Eq. (2.12)]. The growth of *connected* hydrate structures appears thus to be thermodynamically more favorable than an uncorrelated ''through solution'' precipitation mechanism.

On the other hand, in the deacceleration period ($t>t_\times$) the hydrate layers surrounding the cement grains increasingly separate the reacting anhydrous cement and water and thus hinder or block further C_3S dissolution. The hydrates are acting in the deaccelerated period as *inhibitors* [negative exponent for the products in Eq. (2.13)]. The reversed role of hydration products during the accelerated and deaccelerated periods appears to be experimentally evident from the foregoing considerations.

A widespread assertion in cement literature is that early hydration is controlled by chemical kinetics compared to the late stage kinetics which are diffusion controlled. We agree with the second assumption that ion diffusion most probably represents the rate controlling step within the deacceleration period. This is in fact strongly indicated by the very low hydration rate at large times in Fig. 2. However, there is no direct indication that the acceleration kinetics is chemically limited. Obviously Eq. (2.12) cannot describe initial nucleation (approximately within the first 15 min) because there exist no products at these times at all ($[B]|_{t_0}=0$). On the other hand the early nucleation period is not accessible by the experimental techniques considered here, so there is no conflict in interpretation. One just has to keep in mind that all experimental data points as well as the power laws extracted from them are beyond the nucleation period.

After the first few minutes of bringing cement and water into contact, the concentrations of ions in solution increase far beyond the equilibrium solubilities, without any precipitaton. This can be understood by viewing the process of heterogeneous nucleation as overcoming a thermodynamic barrier (supersolubility [7]). Being supersaturated, hydrate nucleation happens on the cement grain surfaces [19,18]. At this instant a more or less significant part of the solution is strongly oversaturated with respect to the equilibrium solubility. The further precipitation (growth) of the hydrates can thus be regarded as happening approximately within a spatially uniform oversaturated solution (oversaturated interface layer). This is of concern in so far as the uniformity of initial conditions is crucial to predicting kinetic exponents for diffusion controlled reactions. It also supposes that the nucleation rate tends rapidly to zero as the hydrate microstructure develops further.

The hydrate microstructure has been experimentally classified for a water to cement ratio $w/c=0.47$. Within the first 4 h foil-like microstructure precipitation is reported to happen radially away from the cement grains (typical dimensions <0.5 μm and $x_B<10^{-2}$). Thereafter (<24 h) the formation of a gelatinous layer sourrounding the cement grains has been observed [thickness ≈ 0.5 μm and $x_B(24\text{ h})\approx 0.3$]. Needle like precipitates have also been found. Finally, after several days crumpled interlocking foils are observed (see Fig. 1). It has also been reported that the precipitated microstructure morphologies are strongly influenced by the available interparticle spacings [19]. There is presently no straightforward way to predict or calculate microstructural morphologies for such complex systems; however, recently developed heterogeneous reaction-diffusion models have received considerable interest in this context [20].

The growth of a precipitate is kinematically very complex. The precipitated geometry (microstructure) cannot be predescribed in general beyond the initial conditions but is rather a *result* of the associated interface dynamics. The simplest case is governed by the growth of spherical precipitates of radius R from an initially supersaturated solution of concentration $\bar{c}$. Let $c=c(r)$ denote the particle concentration in the solvent, $c_{s/}$ the particle concentration within the precipitate at the interface, $c_{/s}(R)$ the particle concentration within the solvent at the interface, and D the diffusion coefficient of particles in the solvent. One has from continuity of mass

$$\frac{dR}{dt}=\frac{D}{c_{s/}-c_{/s}(R)}\left(\frac{dc}{dr}\right)_{r=R}. \tag{3.1}$$

This is the equation of motion for the interface (in spherical coordinates). It establishes the direct proportionality between local growth rate and particle current density at the interface. In general, $c_{/s}$ depends on the (local) interface curvature as a consequence of interfacial tension. If the precipitate is not too small one often assumes the zero curvature limit, i.e., $c_{/s}(R)\approx c_{/s}(\infty)$. The most interesting point in Eq. (3.1) is that the gradient of c contains global information about the interface because $c(r)$ is the solution of the (stationary) diffusion equation

$$\Delta c(r)=0 \tag{3.2}$$

obtained under boundary conditions $c(\infty)=\bar{c}$ and $c(R)=c_{/s}(\infty)$. The solution of Eqs. (3.1) and (3.2) is the well known parabolic growth law [1],

$$R^2-R_0^2=2D\frac{\bar{c}-c_{/s}(\infty)}{c_{s/}-c_{/s}(\infty)}(t-t_0). \tag{3.3}$$

Similarly a parabolic solution is also obtained for the growth of a flat interface. More generally, the local growth rate dynamically depends on (at least) two competitive mechanisms, (a) flattening of high curvature regions due to interfacial tension and (b) sharpening of these regions due to preferential diffusive growth at these ''tips.'' Numerical boundary integral methods have been developed in order to study the associated interface dynamics and instability, e.g., see Ref. [21]. For a perturbative treatment see, for example, Ref. [22].

Despite the complexity of the microstructural transformations involved the natural question arises whether there exists at a given time a *typical microstructure* and a *typical mode of growth* within the system.

Suppose the case of a vanishing nucleation rate during precipitate growth. If the precipitating structure grows geometrically in the form of a plate (see the above experimental classification scheme) then the variation in mole fraction of the precipitated phase in time is predicted theoretically for $x_B\ll 1$ as $x_B\sim(t/\tau)^{5/2}$ [1] with τ being a characteristic time scale for the growth [23]. The plate's rim grows at a constant rate while its thickness grows parabolically in time, explaining the exponent 5/2. For $x_B\ll 1$ one can replace the quantity $f(t)$ by $x_B(t)$ in all foregoing considerations. One is led to the conclusion that for early foil-like hydrate growth γ

$=5/2$ and $(\psi-1)/\psi=3/5$ in Eqs. (2.4) and (2.10), respectively. This is in agreement with the considered measurements (see Fig. 2).

What causes the observed slowing down of the hydration process? If a single foil precipitated in a spatially infinite supersaturated solution there would be no obvious reason for a slowing down of the hydration process as there exists no characteristic length scale. However, the case of cement paste considered here is an assembly of small anhydrous cement grains immersed in water. The mean free distance between particles has to be considered as a typical length scale for transport and for the precipitation process ($x_B \ll 1$). The size of the growing flakes cannot exceed this because of spatial hindrance. Hence there must exist a typical time scale $t_\times$ at which the flakes change their mode of growth into thickening only. We interpret this typical time as the crossover time $t_\times \approx 16$ h observed in Fig. 2. Growth of flakes in the thickening only mode is expected to happen parabolically in time for diffusion limited precipitation reactions [1]. Therefore we predict the exponents of the deaccelerated period to be $\delta=1/2$ and $(\psi-1)/\psi=-1$ in Eqs. (2.5) and (2.10), respectively, in agreement with the experimental data of Fig. 2.

With the above assessments we have apparently related the experimentally observed kinetic exponents of the hydration products to microstructural information. Certainly, there is no unique mapping between kinetics and geometry, but this constitutes a complex question in terms of Eqs. (3.1) and (3.2) to be studied in future in its own right.

So far we have restricted our considerations to the case of a water to cement weight ratio $w/c=0.5$. The question arises whether the kinetic exponents are universal and how the observed typical crossover quantities $t_\times$ and $f_\times$ depend on w/c. We show in Fig. 4 experimental (replotted) data for three different w/c ratios. The data do not collapse, which is not surprising because the typical interparticle spacing does depend on w/c. Qualitatively, higher w/c ratios correspond to lower charateristic times $t_\times$ and lower hydrate ''amounts'' $f_\times$. For early times we observe kinetic exponents that do (apparently) depend on w/c. Interestingly, in all cases the kinetic exponents δ for the deacceleration period are close to 1/2. However, we have not studied this in further detail because there are fewer experimental data available than for the standard case $w/c=0.5$.

IV. CONCLUSION

We have reconsidered NMR measurements on the overall hydration kinetics of tricalcium silicate pastes ($w/c=0.5$) In Sec. II B we briefly discussed the conditions for w/c to satisfy in order to allow a meaningful discussion in terms of a global net reaction and its schematic counterpart. In Sec. II C we demonstrated that the time dependent ratio of hydrated and unhydrated silica mole numbers can be well characterized by two power laws in time, $x/(1-x)\sim(t/t_\times)^\psi$. For early times $t<t_\times$ we found an accelerated hydration ($\psi=5/2$) and for later times $t>t_\times$ a deaccelerated behavior ($\psi=1/2$). The crossover time has been estimated as $t_\times \approx 16$ h. We interpreted these results in terms of a global second-order rate equation indicating that (a) hydrates do catalyze the hydration process for $t<t_\times$, (b) they do inhibit hydration for $t>t_\times$, and (c) the value of the associated second-order rate constant is of magnitude 6×10^{-7}–7×10^{-6} $\mathrm{l\,mol^{-1}\,s^{-1}}$. We have argued in Sec. III, by considering the hydration process as a diffusion limited precipitation that the exponents $\psi=5/2$ and $\psi=1/2$ directly indicate a preferentially leaflike hydrate microstructure. This argument was supported by experimental observations of cellular hydrate microstructures for this class of materials.

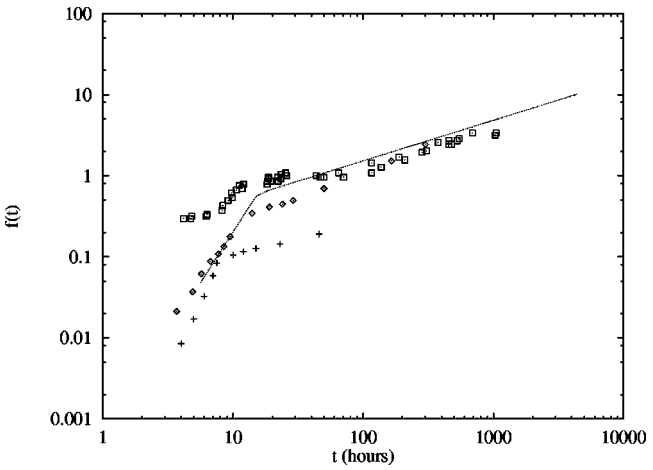

FIG. 4. Same representation as in Fig. 2 but for various water cement ratios employing XDR (x-ray diffraction) and Raman spectroscopy. The measurements were conducted at room temperature and normal pressure. The dashed line shows again the power law fit corresponding to Fig. 2 for comparison purposes. Data from (□) Ref. [10] (Raman, $w/c=0.4$), (◇) Ref. [8] (XDR, $w/c=0.45$), and (+) Ref. [9] (XDR, $w/c=0.7$). Note that the data do not collapse; however, for large times they yield similar slopes $\approx 1/2$ compared to Fig. 2.

ACKNOWLEDGMENTS

F.T. would like to acknowledge financial support from CEC under Grant No. ERBFMBICT 950009 and would like to thank Alex Hansen for his patience during the stay in Trondheim.

[1] V. Raghavan and M. Cohen, in *Changes of State*, Vol. 5 of Treatise on Solid State Chemistry, edited by N.B. Hannay (Plenum Press, London, 1975), pp. 67–127.
[2] G. Sauthoff, J. Phys. IV **6**, 87 (1996).
[3] E.H. Oelkers and P.A. Bjorkum, Am. J. Sci. **296**, 420 (1996).
[4] M.D. Cohen and R.D. Cohen, J. Mater. Sci. **23**, 3816 (1988).
[5] P. Barret and D. Bertrandie, J. Chim. Phys. **83**, 765 (1986).
[6] This is an approximation. A particularity of the cement hydration problem is that the appearing cement hydrate exhibits a variable stoichiometry in the course of its formation (''solid

solution''). The selected stoichiometries in Eq. (2.1) correspond to the late stage proportions in cement hydration [5].
[7] D. Damidot and A. Nonat, Adv. Cem. Res. **6**, 27 (1994).
[8] S. Tsumura, Zement Kalk Gips **11**, 511 (1966).
[9] I. Odler and H. Doerr, Cem. Concr. Res. **9**, 239 (1979).
[10] M. Tarrida, M. Madon, B. Le Rolland, and P. Colombet, Adv. Cem. Based Mater. **2**, 15 (1995).
[11] C.M. Dobson, D.G.C. Goberdhan, J.D.F. Ramsay, and S.A. Rodger, J. Mater. Sci. **23**, 4108 (1988).
[12] A.R. Brough, C.M. Dobson, I.G. Richardson, and G.W. Groves, J. Mater. Sci. **29**, 3926 (1994).
[13] J. Hjorth, J. Skibsted, and H.J. Jakobsen, Cem. Concr. Res. **18**, 789 (1988).
[14] S.U. Al-Dulaijan, G. Parry-Jones, A.-H.J. Al-Tayyib, and A.I. Al-Mana, J. Am. Ceram. Soc. **73**, 736 (1990); H. Justnes, I. Meland, O.J. Bjoergum, and J. Krane, Adv. Cem. Res. **3**, 111 (1990).
[15] J. G. Engelhardt and D. Michel, *High-Resolution Solid State NMR of Silicates and Zerlites* (Wiley, New York, 1987).
[16] Note that $f(t)$ cannot be expressed as the sum of two powers in time because $\gamma > \delta$; compare Eqs. (2.4) and (2.5). However, the time can be expressed as a sum of two powers of $f(t)$.
[17] We assume here a constant and characteristic reference volume V_0. This is an approximation in that the hydrating system Eq. (2.1) undergoes a chemical shrinkage in course of the hydration (nominally 10 Vol %, but in practice less).
[18] H. F. W. Taylor, *Cement Chemistry* (Academic Press, London, 1990).
[19] H.M. Jennings, B.J. Dalgleish, and P.L. Pratt, J. Am. Ceram. Soc. **64**, 567 (1981).
[20] F. Tzschichholz, H.J. Herrmann, and H. Zanni, Phys. Rev. E **53**, 2629 (1996).
[21] D.A. Kessler, J. Koplik, and H. Levine, Adv. Phys. **37**, 255 (1988).
[22] R. Lovett, P. Ortoleva, and J. Ross, J. Chem. Phys. **69**, 947 (1978).
[23] The time scale τ arises from such quantities as initial oversaturation, diffusion coefficients, and water-hydrate interface properties.
[24] T. Knudsen, Cem. Concr. Res. **14**, 622 (1984).